Research Article
doi: 10.1590/01047760202329013265
vol(29), 2023

CERNE

Characterization of the variability of the diameter distribution of natural Taurus cedar stands in Türkiye using Johnson's s_B distribution

Ramazan Özçelik[1]✤, Burak Koparan[1], Teresa J. Fidalgo Fonseca[2], Burak Baş[3]

[1]Isparta University of Applied Sciences, Faculty of Forestry, Türkiye
[2]University of Trás-os-Montes e Alto Douro, Forest Research Centre, School of Agriculture, University of Lisbon, Portugal
[3]Süleyman Demirel University, Graduate School of Natural and Applied Sciences, Türkiye

FOREST MANAGEMENT

ABSTRACT

Background: This article aims to provide information on the diameter distribution of naturally regenerated forests of Taurus cedar (*Cedrus libani* A. Rich), a tree species endemic in the mountains of the Eastern Mediterranean basin and assess their prediction ability with the Johnson S_B distribution. Previous research attested to the flexibility of Johnson family distributions to mimic empirical diameter data for a large set of tree species, justifying its use for the case study. A set of 134 plots (400 m^2) were sampled in the most represented areas of the distribution of the species in Türkiye and diameter at breast height was measured in all the living trees. The cedar forests displayed heterogeneous diameter structures with diameters range from 10 to 116 cm and irregular shapes (e.g. unimodal, bell-shaped, left- and right-skewed, and non-uniform). Over three-quarters of the empirical diameter distributions (104 sample plots) were classified as S_B distribution. The remaining were classified as bounded at the lower end, S_L (16) or unbounded, S_U (14). The authors essayed the 3-parameter and 4-parameter recovery methods after Parresol and Fonseca and other´s fundamental studies. The 3-parameter recovery method outperformed the 4-parameter method in the convergence criterion and error index (EI) expressed in the basal area.

Results: Results show that the Johnson S_B distribution can adequately reproduce the high variability in diameter for most of the distributions observed in these natural forests, providing reliable estimates which can serve as a basis for decision support systems.

Conclusion: The S_B distribution can represent the diameter distributions of natural cedar forests, even if the empirical distributions are not in the region covered by this distribution.

Keywords: Taurus cedar; structural diversity; parameter recovery; stand attributes; forest management

HIGHLIGHTS

Taurus cedar diameter distributions were located in the S_B region, presenting various shapes, from classic bell-shaped, to right or left-skewed, and observations with one or more modes.
The diameter distributions of Taurus cedar in natural stands follow an S_B distribution and can be properly described using a parameter recovery strategy.
Three parameters of the S_B distribution has shown to fit reasonably well most of the observed diameter distributions classified as lower bounded (S_L) or unbounded (S_U).
The estimates of S_B distribution represents the diameter distributions of natural cedar forests.

ÖZÇELIK, R.; KOPARAN, B.; FONSECA, T. J. F.; BAŞ, B. Characterization of the variability of the diameter distribution of natural Taurus cedar stands in Türkiye using Johnson's S_B distribution. CERNE, v.29, e-103265, doi: 10.1590/01047760202329013265

✤Corresponding author: ramazanozcelik@isparta.edu.tr Received: May 12/2023 Accepted: September 6/2023

Open Access
CERNE
ISSN 0104-7760
UFLA UNIVERSIDADE FEDERAL DE LAVRAS

INTRODUCTION

Sustainable Development Goal (SDG 15) by United Nations spells out the importance of protecting, restoring, and promoting sustainable management of all types of forests, with specific targets on protecting biodiversity and natural habitats and ensuring the conservation of mountain ecosystems. To this end, knowledge of natural forests' current condition and characteristics is essential. Taurus cedar (*Cedrus libani* A. Rich), also called Lebanon cedar, is a highly significant and widespread forest tree species in Türkiye, covering a vast forested region of about 402,000 hectares and holding a current standing volume of roughly 30 million cubic meters (GDF, 2020). The species is presently found primarily in the Taurus Mountains of Türkiye (Boydak, 2007), where generally occurs between 800 and 2100 m in elevation. The species can be found at lower (500-600 m) and higher (2400 m) elevations as small populations or small groups and individuals (Boydak, 2003).

Taurus cedar is the most essential and valuable conifer species economically for the forest products industry in Türkiye due to its high-quality wood (Bozkurt et al., 1990). Furthermore, Taurus cedar forests play a key role in providing important benefits and environmental services such as protecting soil and water resources and conserving biological diversity in the Taurus Mountains. Therefore, efficient management planning of the multipurpose forestry of Türkiye requires tools capable of considering the structures and specific characteristics of cedar forests. In this context, information on the stand forest structure is critical to improving knowledge about species development and supporting forest management and timber resource planning strategies (Hafley and Schreuder, 1977; Cao et al., 2010; Lima et al., 2017; Ciceu et al., 2021). The structure study can be accomplished through the horizontal distribution of tree size, with the diameter at breast height (*d*) being the most used variable. As indicated (Sun et al., 2019), diameter is generally related to other essential variables, including basal area, density, and volume. Therefore, the diameter distribution model is a powerful tool to provide more detailed information about the stand without additional inventory costs (Nord-Larsen and Cao, 2006; Bergseng et al., 2015).

In the context of timber production, knowing about the diameter distribution of trees is crucial for predicting future timber product volumes and quality standards. Similarly, in the management of wildlife habitats, understanding the diameter distribution of a stand can offer valuable information about its structure and suitability for supporting different types of wildlife species (Bankston et al., 2021). Zhang et al. (2003) suggest that one way to meet these information requirements is by employing diameter distribution models, which employ a probability density function (PDF) to allocate a stand attribute over size classes, such as diameter classes. Many different PDFs have been used to describe diameter distribution in a forest stand, such as log-normal, exponential, gamma, beta, Johnson's S_B, and Weibull functions (Liu et al., 2009).

Among many PDFs, the S_B distribution, proposed by Johnson (Johnson, 1949) is one of the most commonly chosen for modelling diameter distributions in forestry practices (Hafley and Schreuder, 1977; Scolforo and Thierschi, 1998; Kiviste et al., 2003; Zhang et al., 2003; Parresol, 2003; Scolforo et al., 2003; Siipilehto and Siitonen, 2004; Furtado, 2006; Lei, 2008; Fonseca et al., 2009; Mateus and Tomé, 2011; Cosenza et al., 2019; Sakıcı, 2021; Sakıcı and Dal, 2021; Özçelik et al., 2022), due to its well-recognized flexibility to simulate empirical distributions. The S_B distribution covers a large part of (β_1, β_2) skewness squared and kurtosis´s space, making it particularly apt to describe various distribution curves. The region in the space (β_1, β_2) not enclosed by the S_B is covered by Johnson's S_L distribution (L, from bounded at the lower end) or S_U distribution (U, from unbounded), or corresponds to combinations of β_1 and β_2 that are mathematically impossible of occurring (above the line defined by $\beta_1 - \beta_2 = 0$). The fact that the S_B has bounds at both ends is considered an additional advantage for describing tree diameter distributions because those distributions have defined values at both extremes (minimum and maximum diameter values).

The parameters of the S_B distribution can be estimated using linear and nonlinear regression methods, the percentile method, moments, and maximum likelihood. Parresol et al. (2010) stated that parameter recovery is the state-of-the-art approach for parameter estimation in growth and yield modeling. Better results are obtained through a parameter recovery approach than the parameter prediction approach (Fonseca et al., 2009). Parresol (2003) presented a loblolly pine (*Pinus taeda*) growth-and-yield model using the S_B distribution, where one distribution parameter was fixed, and the remaining three parameters were estimated in a parameter-recovery context from the median, the average, and the minimum diameter (in cm) of the observed diameter distribution. The methodology of Parresol was more general than previous S_B-based growth and yield models, which recovered only one or two parameters (Newberry and Burk, 1985; Scolforo and Thierschi, 1998). Fonseca (2004) and Fonseca et al. (2009) extended the three-parameter recovery method (3-PRM) to create a scheme that completely recovers Johnson's S_B diameter distribution from stand variables, the four-parameter recovery method (4-PRM). The 4-PRM model includes, as an additional stand variable, the third non-central moment of diameter distribution. This method has compared favorably to the 3-PRM for maritime pine diameter distributions, encompassing unimodal, decreasing, and bimodal shapes and non-definite diameter distribution shape. Recent advances with full-non-conditioned maximum likelihood estimation (FMLE) (Özçelik et al., 2016) have provided a good performance of both 4-parameter estimation methods for Brutian pine. The FMLE uses all the available observations of individual diameters of the trees, whereas the 3-PRM and the 4-PRM are supported by summaries of the diameter data; such as mean, median, and basal area. This feature puts parameter recovery-based methods at an advantage when the goal is to reduce the data required for simulation, which is undoubtedly an important feature to consider when combining diameter distributions with growth and yield models.

The purpose of this study is two-fold: (1) to describe and characterize the empirical diameter distributions of natural stands of Taurus cedar in the Mediterranean Region

of Türkiye and (2) to evaluate the adequacy of the Johnson S_B distribution based on parameter recovery methods (3-PRM and 4-PRM) to describe the empirical diameter distributions of natural forests of Taurus cedar that can be useful to support volume and carbon stock assessment of cedar forests. The authors hypothesized that the diameter distributions of Taurus cedar natural stands follow an S_B distribution and can be properly described using a parameter recovery approach.

MATERIAL AND METHODS

The study area

The required data for this study was gathered from 134 sample plots located in pure natural and even-aged Taurus cedar stands in the Mediterranean Region of Türkiye. The study area had various plots that were chosen in a subjective manner to reflect the diverse range of ages, densities, and locations of the stands. The sample plots were circular, and their size varied from 200 to 4000 m^2, depending on the density of the stand, to ensure at least 30 trees were present in each plot. To calculate the diameter at breast height (d, cm), two perpendicular diameters outside-bark were measured on each tree at 1.3 m above the ground and then averaged arithmetically. Dominant diameter (d_{dom}) was calculated from the percentage of the 100 thickest trees per ha. Taurus cedar distribution on Türkiye and the study area shown in Figure 1.

Probability density function modeling

Most of the studies (Table 1) describe empirical bell-shaped distributions with some degree of asymmetry, many of which relate to planted forests. In the case of natural forests, the diameter distributions should display higher variability in both shape and tree size, notably when there is irregularity also in tree age. The scarcity of studies concerning complex structures can be at least partially explained by the fact that the description of diameter distributions with theoretical functions, even when they are flexible to suit variable shapes, is usually attempted with more regular shapes that are easier to describe. Table 1 summarizes the studies using theoretical distributions to express empirical diameter distributions, with the identification of the tree species, the shape of diameter distribution, stand age range, and type of regeneration (natural or plantations).

The S_B probability density function (PDF) for a x variable ($x \in (\xi, \xi + \lambda)$) is defined in equation [1]. The distribution has 4 parameters ξ, λ, δ and γ. The parameter ξ ($-\infty < \xi < -\infty$) represents the lower end, λ is the range parameter (with the upper bound being defined by ξ + λ), and the δ and γ control the shape of the distribution.

$$f(x) = \frac{\delta\lambda}{\sqrt{2\pi}(x-\xi)(\xi+\lambda-x)} exp\left(-\frac{1}{2}\left(\gamma + \delta ln\left(\frac{x-\xi}{\xi+\lambda-x}\right)\right)^2\right) \quad (1)$$

where λ, δ > 0, ξ < x < ξ + λ, , and -∞ < γ < -∞.

The following variables were calculated from each plot: average diameter at breast height ($\bar{d}$), quadratic mean diameter (dg), dominant diameter (d_{dom}), minimum diameter (d_{min}), maximum diameter (d_{max}), median diameter ($d_{0.50}$), number of trees per hectare (N), and stand basal area (G). Table 2 presents a summary of key variables, such as mean, maximum, minimum, and standard deviation (SD) values. Also provided is the characterization of the estimated skewness ($\sqrt{b_1}$) and kurtosis (b_2) of the empirical diameter distributions.

The estimated skewness $\sqrt{b_1}$ values ranged between -1.11 and 3.6, with negative values being typically associated with a longer tail on the left side of a unimodal distribution while positive values refer to a longer tail on the right. The estimated kurtosis values ranged between -1.22 and 18.5. For kurtosis, negative values indicate distributions with lighter tails than normal, while positive values indicate distributions with heavier tails. A kurtosis value greater than the typical 3.0 for a standard normal deviation suggests a leptokurtic distribution. The distribution of the average, median and extreme diameter values for the 134 observations and how these variables relate is depicted in Figure 2.

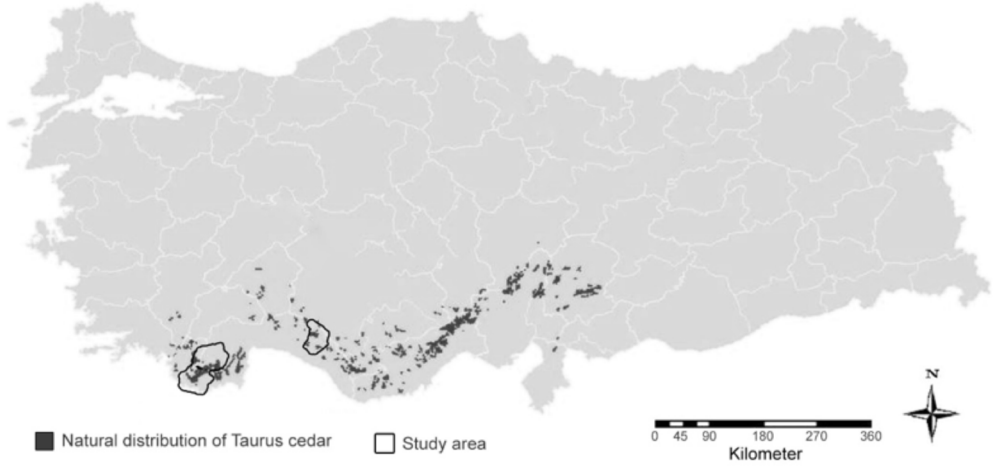

Figure 1: Taurus cedar distribution in Türkiye and sampled areas.

Table 1: An overview of diameter distribution studies using PDFs.

References	Species	Shaped	Ranged age	Natural forests or plantation
Bailey and Dell, 1973	*Pinus banksiana*	Bell-shaped	55	n.a.
Mowrer, 1986	*Populus tremuloides*	Bell-shaped - Right skewed	1-130	Natural
Kamziah, 1998	*Acacia mangium*	Bell-shaped	2-22	Plantation
Scolforo et al., 2003	*Pinus taeda*	n.d.	3-10	Plantation
Fonseca, 2004	*Pinus pinaster*	Regular shaped and non-uniform	12 - 70	Natural and Plantation
Nord-Larsen and Cao, 2006	*Fagus sylvatica*	Bell-shaped – Right skewed	1-140	Natural
Borders et al., 2008	*Pinus elliottii*	Bell-shaped	17-24	Plantation
Lei, 2008	*Pinus tabulaeformis*	n.d.	n. a.	Plantation
Fonseca et al., 2009	*Pinus pinaster*	Bell-shaped	n. a.	Plantation
Mateus and Tomé, 2011	*Eucalyptus globulus*	Bell-shaped	1-24	Plantation
Bergseng et al., 2015	*Picea* sp., *Pinus* sp.	Bell shaped – Right Skewed	n.a.	Natural
de Lima et al., 2015	n.a	Bell-shaped	n. a.	Natural
Özçelik et al., 2016	*Pinus brutia*	Bell-shaped	29-95	Natural
Ogana et al., 2017	*Gmelina arborea*	Bell-shaped	11-32	Plantation
Arias-Rodil et al., 2018	*Pinus radiata*	n.d.	12-41	Plantation
Ezenwenyi et al., 2018	*Nauclea diderrichii*	Bell-shaped	42-46	Plantation
Maltamo et al., 2018	*Eucalyptus urograndis*	Bell-shaped – Left skewed	2-12	Plantation
Mayrinck et al., 2018	*African mahogan*	Bell-shaped	1-14	Plantation
Pogoda et al., 2019	*Alnus glutinosa*	Bell-shaped	20-80	n. a.
Cosenza et al., 2019	*Pinus radiata*, *Eucalyptus globulus*	Bell-shaped	n. a.	Plantation
Sun et al., 2019	*Pinus tabulaeformis*, *Pinus armandii*, *Quercus aliena*	Bell-shaped- Right skewed	n. a.	Natural
Pogoda et al., 2020	*Alnus glutinosa*	Bell shaped	20-80	n. a.
Gorgoso-Varela et al., 2020	*Eucalyptus globulus*, *Pinus radiata*, *Gmelina arborea*	Bell-shaped	2-41	Plantation
Adedoyin et al., 2021	*Parkia biglobosa*	Bell-shaped	n.a.	Plantation
Bankston et al., 2021	*Pinus taeda*	n.d.	8-31	Plantation
Ciceu et al., 2021	*Picea* sp., *Pinus* sp., *Abies* sp.	n.d.	n. a.	Natural
Özçelik et al., 2022	*Quercus cerris*, *Quercus petrae*, *Quercus frainetto*	Bell shaped Right- skewed	None	Natural
Sakıcı, 2021	*Abies nordmanniana* subsp. *equi-trojani*	n.d.	n. a.	Natural
Sakıcı and Dal, 2021	Pinus sylvestris	n.d.	n. a.	Natural
Vega et al., 2022	*Alnus* sp., *Arbutus* sp., *Quercus* sp., *Pinus* sp., *Juniperus* sp.	Irregular shaped	n. a.	Natural

Note: n.d. not determined, n. a. not available.

Table 2: Stand characteristics of the observed diameter distributions of Taurus cedar in Türkiye.

Variables	Mean	Minimum	Maximum	SD
$\bar{d}$ (cm)	21.3	5.9	41.1	7.3
dg (cm)	45.5	24.3	64.1	8.1
$d_{0.50}$ (cm)	21.3	5.0	43.0	7.8
d_{min} (cm)	5.5	2.0	12.0	1.8
d_{max} (cm)	46.2	14.0	120.0	16.4
d_{dom} (cm)	39.6	11.8	71.8	12.3
G (m^2 ha^{-1})	31.1	6.2	65.6	10.1
N (trees ha^{-1})	1022.9	192	5600	874.8
Skewness ($\sqrt{b_1}$)	0.4	-1.1	3.6	0.6
Kurtosis (b_2)	0.5	-1.2	18.5	2.3

Note: $\bar{d}$, average diameter; *dg*, quadratic mean diameter; $d_{0.50}$, median diameter; d_{min}, minimum diameter; d_{max}, maximum diameter; d_{dom}, dominant diameter; *G*, stand basal area; *N*, number of trees per hectare; $\sqrt{b_1}$ estimated skewness; b_2, estimated kurtosis.

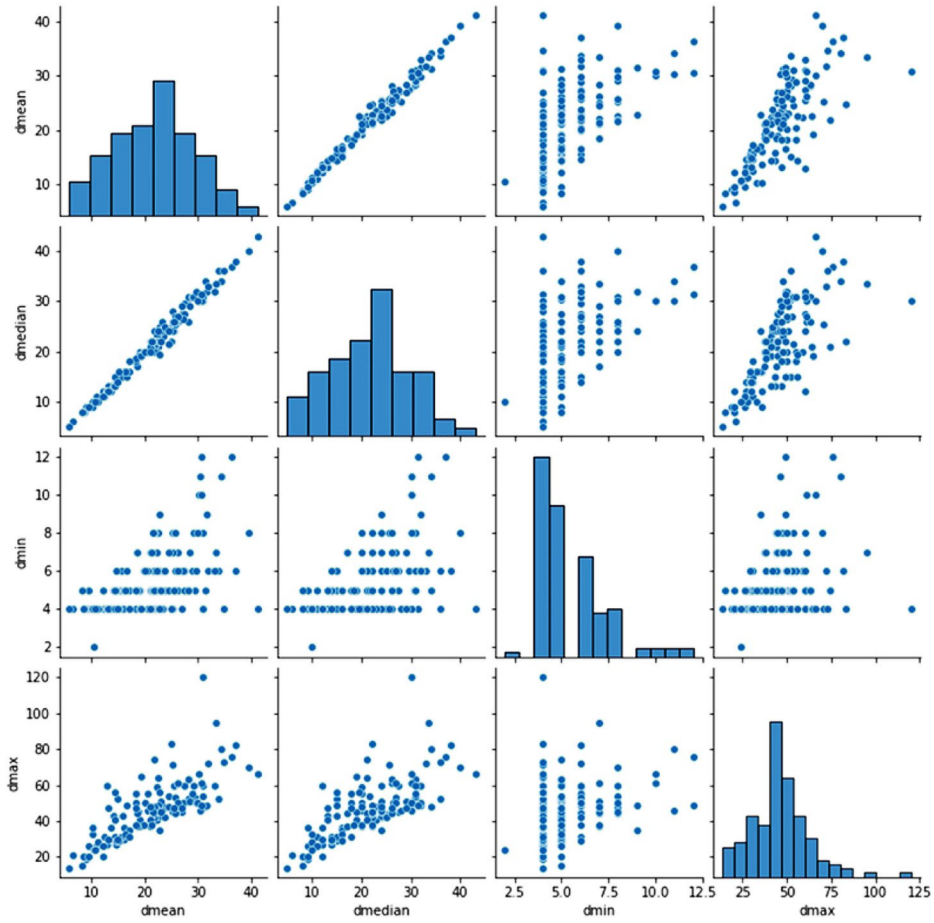

Figure 2: Distribution of average, median, minimum and maximum diameter values for the dataset (n = 134).

To solve the 3-PRM and the 4-PRM, we followed the methodology presented by Parresol et al. (2010). The 3-PRM and the 4-PRM approaches are described through the transformed *x* values as $y = (x - \xi)/\lambda$, where the *x* variable represents *d*. In the 3-PRM the location parameter ξ is specified outside of the system, and equations 2, 3, and 4 constitute the system to recover the range and the shape parameters (three equations for three unknowns). Briefly, the relationship [2], where $y_{0.50}$ denotes the median of *Y*, is used to eliminate γ [3] and [4]. The system reduces then to three nonlinear equations for an equal number of unknowns.

$$\gamma = \delta \ln\left(\frac{1}{y_{0.50}} - 1\right) \quad (2)$$

$$\bar{d} = \xi + \lambda \mu_1'(y) \quad (3)$$

$$G = kN\left[\xi^2 + 2\xi\lambda\mu_1'(y) + \lambda^2\mu_2'(y)\right] \quad (4)$$

The equation [3] expresses average tree diameter ($\bar{d}$) as a function of the first noncentral moment of Y (μ_1') whereas equation 4 expresses stand basal area (G) as a function of the first two noncentral moments of Y (μ_1' *and* μ_2'). In [4], the variable N represents the number of trees per unit area and k is a conversion factor (π/40 000). In the 4-PRM, the system is constituted by equations [2], [3] and [4], complemented with an additional equation [5]. Using equations [2] to [5], the system reduces to four nonlinear equations for an equal number of unknowns, avoiding the *a priori* specification of the location parameter. Equation [5] expresses the product of the mean of the basal area-sized distribution of tree diameters ($\bar{d}_G$) by the square of the quadratic mean diameter, variable dg, as a function of the first three non-central moments of y. The variable $\bar{d}_G$ is calculated as a weighted mean of the stand diameters using as the weight function the individual basal area values. For further details, see Fonseca et al. (2009) and Parresol et al. (2010).

$$\bar{d}_G dg^2 = \xi^3 + 3\xi^2\lambda\mu_1'(y) + 3\xi\lambda^2\mu_2'(y) + \lambda^3\mu_3'(y) \quad (5)$$

Model performance

The SAS program was applied to recover parameters for the input of the initial stand conditions (SAS Institute, 2010). After recovering the parameters, the empirical and the estimated diameter distributions were visually depicted. Model adequacy of the parameter recovery approach was evaluated by the analysis of the goodness-of-fit using 5-cm wide diameter classes. The metric selected for the assessment was the error-index (EI), as suggested by Reynolds et al. (1988) and previously followed by other authors in similar studies. For each diameter distribution, the EI was computed as the sum of the absolute deviations of the class basal areas [6] where $\hat{G}_j$ and G_j are the estimated and the observed values of basal area of diameter class j (j = 1 to k), respectively. Calculations of EI were performed for the solutions achieved with the 3-PRM and the 4-PRM.

$$EI = \sum_{(j=1)}^{k} [\hat{G}_j - G_j] \quad (6)$$

RESULTS

Localization of the empirical distributions in the (β_1, β_2) space

Information of estimated skewness ($\sqrt{b_1}$) and estimated kurtosis (b_2) was used to represent the 134 observations in the (β_1, β_2) space of skewness squared and kurtosis to assess whether the empirical distributions were from the S_B family of distributions (Figure 3). The combinations of estimated skewness and kurtosis corresponding to the S_L distribution are identified by the line designated as the S_L curve. The S_B distribution occupies the region between the two reference lines. The region below the S_L corresponds to the Johnson's S_U distribution. According to the estimated values of ($\sqrt{b_1}$, b_2), 104 empirical distributions out of the 134 are in the S_B region (with a few close to the S_L region), and the remaining 30 are in the SL line (16) or in the S_U region (14). This result means that the majority of the Taurus cedar diameter distributions (approximately 80 percent of the sampled forests' diameter distributions) can be described by the Johnson's S_B distribution.

Estimation of the distributions and assessment of goodness-of-fit

Convergent solutions were obtained for the complete data set for the 3-PRM, representing convergence rates of 100%. For the 4-PRM, 28 observations did not present a convergent solution. Table 3 summarizes the results of goodness-of-fit as evaluated by the Error Index (EI) for the global data set, discriminated by distribution family and parameter recovery approach.

Since the employment of non-optimal solutions could distort the performance of the 4-PRM, the EI was re-analyzed focusing on the 104 cases in which the 4-PRM resulted in a convergent solution (Table 4).

A subset of the sampled distributions corresponding to the three types, S_B, S_L and S_U are shown in Figures 4 to 6. For each distribution family, we choose four to six examples representing various shapes and different levels of error values. In Figure 4, observation P61 is a right-skewed unimodal fit, with both parameter recovery approaches presenting excellent fit (with a non-optimal solution for the 4-PRM, as convergence was not met). Observation P112 is right-skewed, and observation P46 shows reasonable bimodal fits to the observed frequencies. Observation P35 is a left-skewed unimodal fit. Observations P59 and P32 have irregular shapes, with P59 resembling bimodal and P32 close to platykurtic distribution, with a lower peak and longer tails than a normal distribution. The 4-PRM fits the bimodal shape in P59. In P32, the 3-PRM shows a better fit than the 4-PRM. In Figure 5, observation P47 resembles the normal distribution, showing a slight deviation from the normal distribution. Observed diameter distribution P16 is skewed to the right and shows two modes in the 5-cm class distribution representation that the parameter recovery methods do not explicitly estimate. For the 4-PRM the fit corresponds to a non-optimal solution. Observations P83 and P23 have irregular shapes, with the 3-PRM presenting bimodal fits to the observed frequencies. In observation P83, the estimated distributions do not encompass the observed diameter range. For the distributions identified in Figure 6, observations P123 and P120 have some resemblance with the bell shape despite the degree of asymmetry to the right. Observations P3 and P129 depict

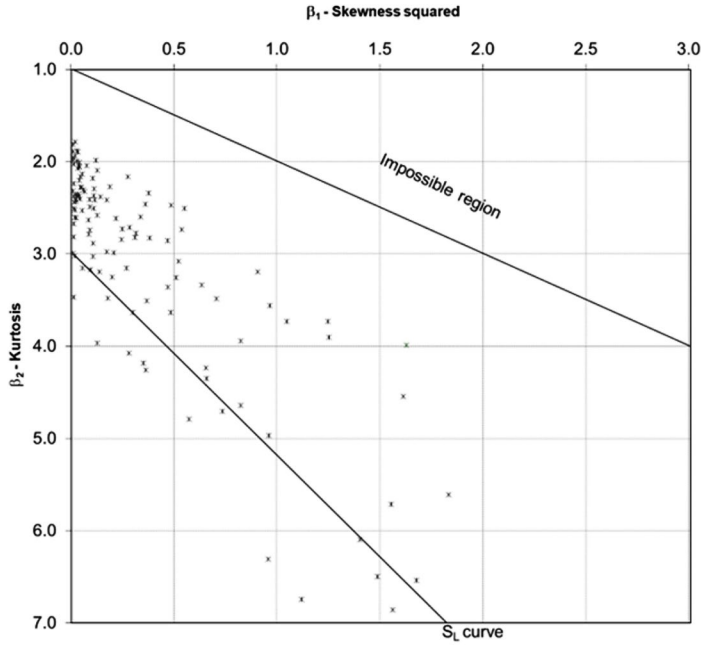

Figure 3: Representation of the n = 134 observations in the (β_1, β_2) space of skewness squared and kurtosis.

Table 3: Statistical evaluation of the goodness-of-fit of the estimated diameter distributions based on the recovery approach 3-PRM and 4-PRM (n = 134).

Distribution:	S_B		S_L		S_U		All	
EI	3-PRM	4-PRM	3-PRM	4-PRM	3-PRM	4-PRM	3-PRM	4-PRM
n	104	104	16	16	14	14	134	134
Median	11.6	11.5	14.0	18.9	13.4	20.5	12.1	13.2
SD	7.6	18.6	5.9	10.9	6.1	18.9	7.3	18.0
# best	55	49	9	7	12	2	76	58

Note: EI, Error index (m^2/ha); SD, Standard deviation; # best, Number of cases where the value of the metric IE was lower than that obtained with the alternative method.

Table 4: Statistical evaluation of the goodness-of-fit of the estimated diameter distributions based on the recovery approach 3-PRM and 4-PRM, restricting the analysis to the subset of data that presented a convergent solution with the 4-PRM (n = 106).

Distribution:	S_B		S_L		S_U		All	
EI	3-PRM	4-PRM	3-PRM	4-PRM	3-PRM	4-PRM	3-PRM	4-PRM
n	84	84	11	11	11	11	106	106
Median	11.0	11.1	12.0	15.8	13.3	19.4	11.8	12.2
SD	6.5	18.7	5.3	11.5	5.2	19.6	6.3	18.2
# best	47	37	5	6	9	2	61	45

Note: EI, Error index (m^2/ha); SD, Standard deviation; # best, Number of cases where the value of the metric IE was lower than that obtained with the alternative parameter recovery method.

irregular shapes, with both recovery methods presenting a reasonable fit in the former. In P129, the goodness-of-fit to the observed distribution is lower, namely with the 4-PRM, which estimates two out-of-place modes. The 3-PRM fit resembles a uniform distribution, which is by far more in accordance with the observed shape of the diameter distribution in the stand.

DISCUSSION

The representative database of Taurus cedar diameter distributions, in a total of 134 sampled natural forests in Türkiye, exposed a wide variety of shapes of the distribution of trees by diameter classes, unimodal with different degrees of asymmetry and kurtosis, and

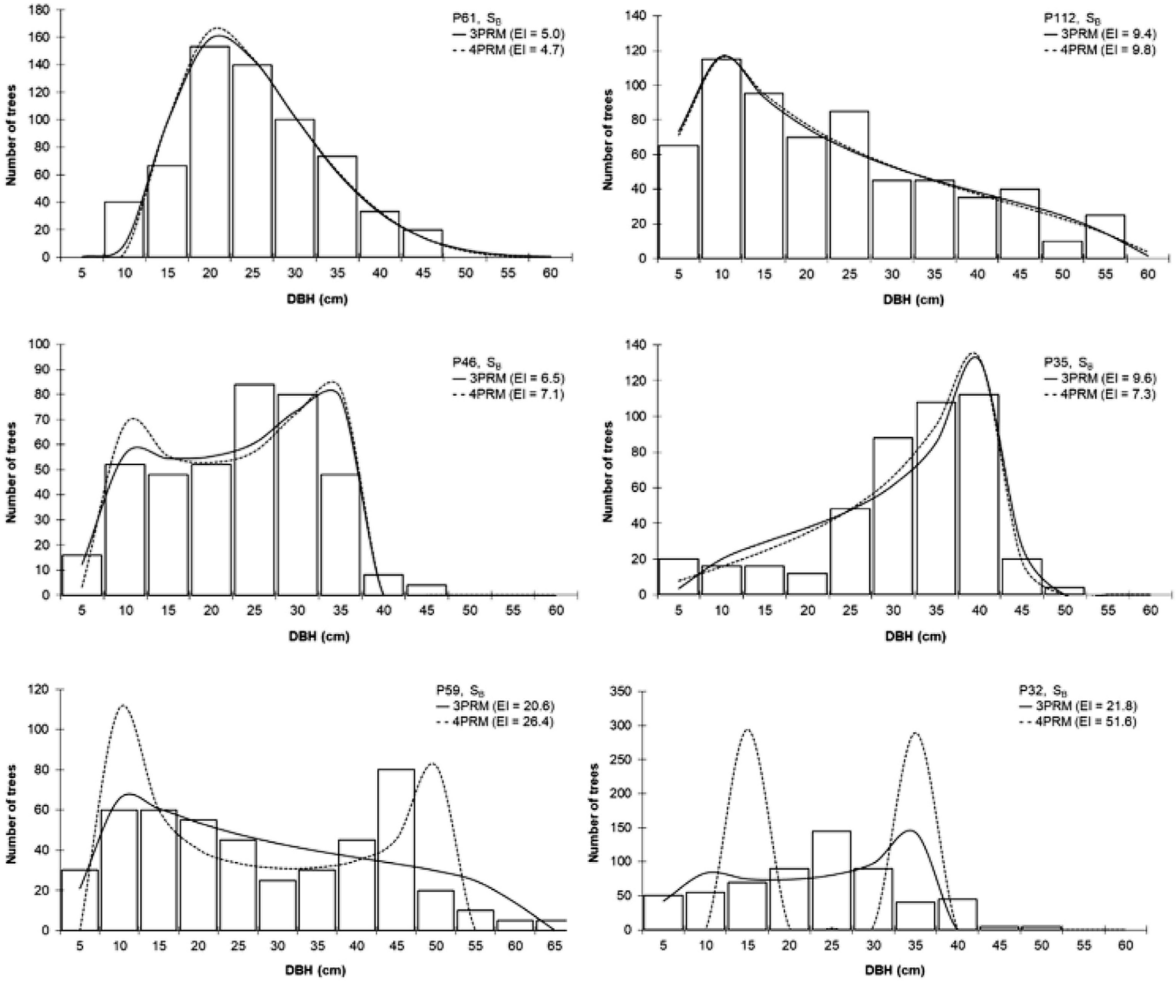

Figure 4: Empirical distributions classified as Johnson' S_B. Observed frequencies and S_B simulated distributions.

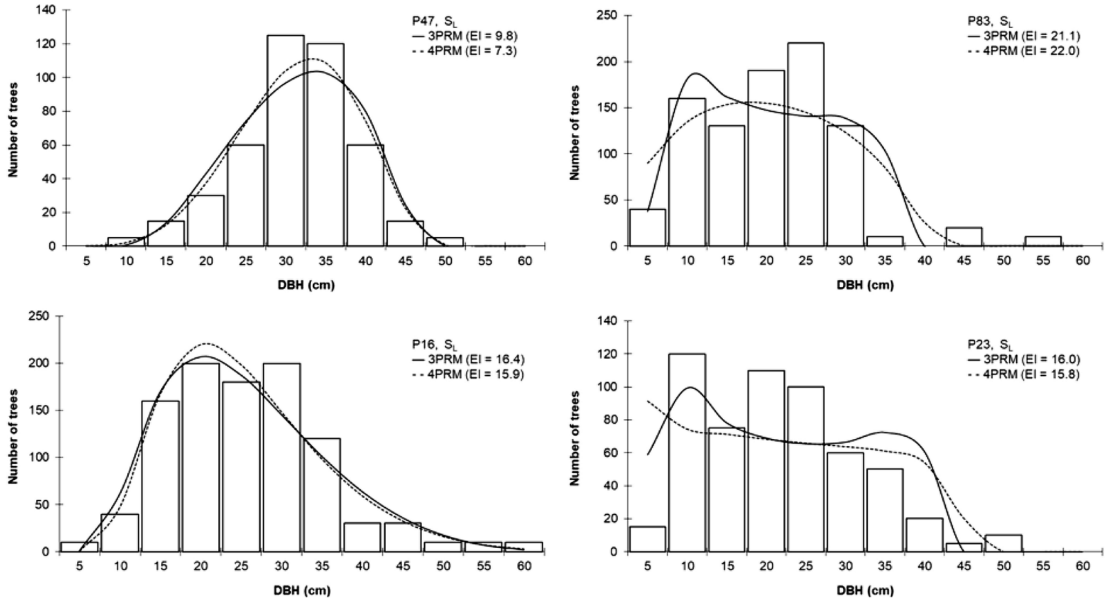

Figure 5: Empirical distributions classified as Johnson' S_L. Observed frequencies and S_B simulated distributions.

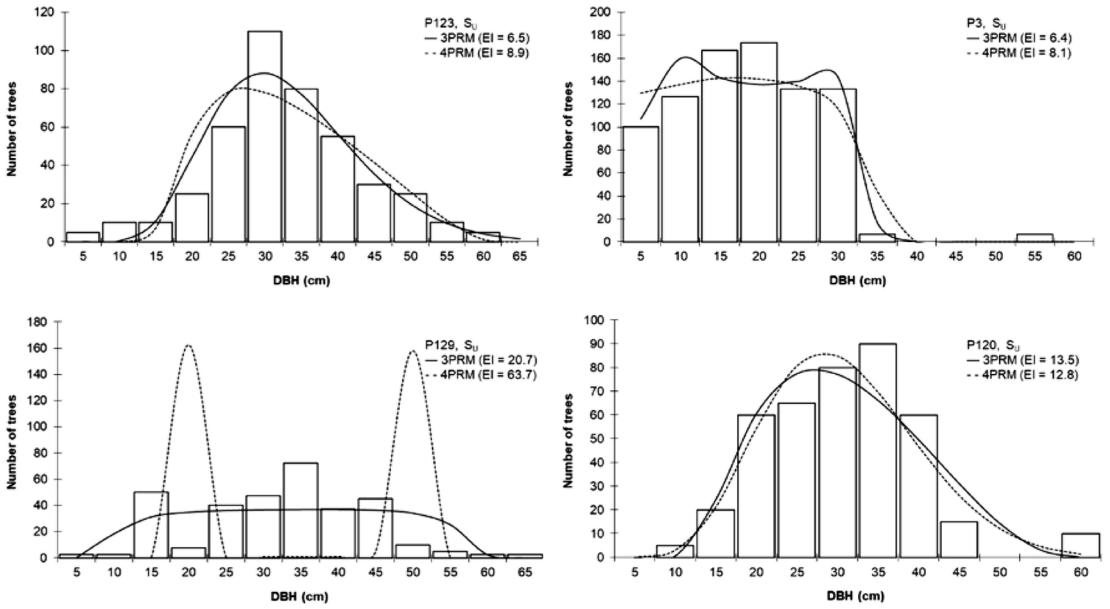

Figure 6: Empirical distributions classified as Johnson' S_U. Observed frequencies and S_B simulated distributions.

bimodal, as well as wide ranges of diameter variation (see Figures 4 to 6, for an overview). The statistical analysis of skewness and kurtosis and depiction of the estimated values in the (β_1, β_2) space showed that most of the cedar diameter distributions are in the region covered by Johnson's S_B distribution. This result confirms the flexibility of S_B distribution to describe the diameter distributions of forest species as noticed in previous studies (e.g., Kamziah, 1998; Scolforo and Thierschi, 1998; Fonseca, 2004; Borders et al., 2008; Fonseca et al., 2009; Mateus and Tomé, 2011; Özçelik et al., 2016; Ogana et al., 2017; Sakıcı and Dal, 2021). The use of PDFs to describe diameter distribution in natural forests has not been reported as frequently as its use in plantations, with more regular diameter distributions, as noticed in Table 1. The results here presented substantiates the adequacy of the S_B distribution to describe diameter distributions in forests where irregular diameter distributions occur.

In this case study, the parameters of the S_B distribution were obtained using the parameter recovery approach. Previous studies corroborate the adequacy of the 3-PRM proposed by Parresol and have highlighted a comparable behavior with the recovery of the 4 parameters that define the distribution (e.g., Fonseca, 2004; Fonseca et al., 2009). In the current study, the results achieved with the 4-PRM did not perform as anticipated, in terms of convergence.

Unsuccessful termination with the number of iterations exceeded or achievement of local minima, was previously reported by Arias-Rodil et al. (2018) for 4-PRM. As stated by Parresol et al. (2010), the S_B parameter recovery approach involve solving complex systems of nonlinear equations. Analysis of the effect of non-optimal solutions on the goodness-of-fit did not show evidence that justifies the exclusion of the estimates with the 4-PRM on those situations. For the 104 observations with convergent solution, the median EI value was slightly lower (EI = 12.2 m^2ha^{-1}, instead of 13.2 m^2ha^{-1} for the 134 observations), but the method performed similarly to what was achieved with the full data set. We conclude that, in general, the goodness-of-fit obtained with the 4-PRM using the optimal or non-optimal solutions are similar, with the convergence criterion not being a relevant factor in utilizing the 4-PRM. As this interpretation is case study-based, more research should be done to confirm that the solutions from the 4-PRM can be used even when they are not the optimal solutions. A case study by Cosenza et al. (2019) on diameter distributions prediction based on airborne laser scanning data mentions that Jonhson´s S_B PDF is more flexible than the Weibull function but also more sensitive to possible errors arising from the higher number of stand variables needed to estimate the PDF parameters. Independently of the strategy used to obtain the values of the parameters (estimation or recovery) there is usually a trade-off between the flexibility to mimic reality (performance effectiveness) and the number of parameters in the PDF. Moreover, the greater the number of parameters estimated outside the system, the greater the possibility of obtaining a good quality fit of the theoretical PDF to the real data. The option to use the 3-PRM, where the location parameter (ξ) is a priori specified or to use the 4-PRM exemplifies another trade-off between a computationally less complex system (ease-of-use) and a method that recovers all four parameters inside the system, i.e., from stand variables. An alternative method that has also provided good results is the non-conditional maximum likelihood estimation (FMLE) by Özçelik et al. (2016). The major advantage of the 4-PRM (that also applies to the 3-PRM) over the FMLE relies on the reduced level of input information required. This is a relevant factor when aiming to project the distribution of diameters or to combine the description of the distribution with growth models, albeit

caution should be exercised when modeling variables that may exhibit strong relationships between them, as is the case of the median and mean of the observed diameter distribution (Figure 2). In a few cases, it has been noticed that the 4-PRM results in bimodal shapes, non-conforming to the empirical distributions (e.g., observation P129 in Figure 6). The reduced number of cases depicted in the dataset was insufficient to identify the causes, however this fact should be considered in future research.

Regarding the estimation of empirical distributions of Taurus cedar that were not located in the region of the (β_1, β_2) space covered by the S_B distribution, the estimates obtained with the 3-PRM have shown to conform to the observed diameter distributions classified as being lower bounded (S_L) or unbounded (S_U). The 4-PRM has described properly some of those empirical distributions (Tables 3 and 4, Figures 5 and 6), but, overall, the 3-PRM performs better for observations out of the S_B region.

CONCLUSIONS

Far more than three-quarters of the Taurus cedar diameter distributions were located in the S_B region, presenting various shapes, from classic bell-shaped, to right or left-skewed, and observations with one or more modes. The results achieved in this study support the hypothesis that the diameter distributions of Taurus cedar in natural stands follow an S_B distribution and can be properly described using a parameter recovery strategy. Moreover, the method that recovers the three parameters of the S_B distribution has shown to fit reasonably well most of the observed diameter distributions classified as lower bounded (S_L) or unbounded (S_U). This result suggests that the estimates obtained with the S_B distribution can represent the diameter distributions of natural cedar forests, even if the empirical distributions are not in the region covered by this distribution.

AUTHORSHIP CONTRIBUTION

Project Idea: RO, BK, TF, BB

Funding: RO, BK, TF, BB

Database: RO, BK, TF, BB

Processing: RO, BK, TF, BB

Analysis: RO, BK, TF, BB

Writing: RO, BK, TF, BB

Review: RO, BK, TF, BB

ACKNOWLEDGEMENTS

This research was financially supported by the Süleyman Demirel University Scientific Research Projects Coordination Unit with the Project Number BAP-4753-YL1-16.

REFERENCES

ADEDOYIN, E. D.; ADEOTI, O. O.; AWOSUSI, B. M.; ONILUDE, Q.; AINA-ODUNTAN, O. A. Evaluating diameter distribution model of *Parkia biglobosa* plantation (Jacq.) G. Don in Wasangare, Saki West Local Government Area of Oyo State, Nigeria. Journal of Forestry Research and Management, v. 18, n. 3, p198-206 2021.

ARIAS-RODIL, M.; DIÉGUEZ-ARANDA, U.; ÁLVAREZ-GONZÁLEZ, J. G.; PÉREZ-CRUZADO, C.; CASTEDO-DORADO, F.; GONZÁLEZ-FERREIRO, E. Modeling diameter distributions in radiata pine plantations in Spain with existing countrywide lidar data. Annals of Forest Science, v. 75, p. 1-12, 2018.

BAILEY, R. L.; DELL, T. Quantifying diameter distributions with the Weibull function. Forest Science, v. 19, n. 2, p. 97-104, 1973.

BANKSTON, J. B.; SABATIA, C. O.; POUDEL, K. P. Effects of sample plot size and prediction models on diameter distribution recovery. Forest Science v. 67, n. 3, p. 245-255, 2021.

BERGSENG, E.; ØRKA, H. O.; NÆSSET, E.; GOBAKKEN T. Assessing forest inventory information obtained from different inventory approaches and remote sensing data sources. Annals of Forest Science, v. 72, p. 33-45, 2015.

BORDERS, B. E.; WANG, M.; ZHAO, D. Problems of scaling plantation plot diameter distributions to stand level. Forest Science v. 54, n. 3, p. 349-355, 2008.

BOYDAK, M. Reforestation of Lebanon cedar (*Cedrus libani* A. Rich.) in bare karstic lands by broadcast seeding in Turkey. In Options méditerranéennes, Series A: Mediterranean Seminars, Ciheam, Italy, 2007, p. 33-43.

BOYDAK, M. Regeneration of Lebanon cedar (*Cedrus libani* A. Rich.) on karstic lands in Turkey. Forest Ecology and Management v. 178, n. 3, p. 231-243, 2003.

BOZKURT, A. Y.; GOKER, Y.; ERDIN, E. Taurus Cedar (*Cedrus libani*) Anatomical and Technological Features. International Cedar Symposium, Forestry Research Institute, Antalya, Turkey, (22-27 October 1990), 1990.

CAO, Q. V.; YAO, F.; WU, Q. Effects of sample size on characterization of wood-particle length distribution. Wood and Fiber Science v. 42, n. 1, p. 46-50, 2010.

CICEU, A.; PITAR, D.; BADEA, O. Modeling the diameter distribution of mixed uneven-aged stands in the south western Carpathians in Romania. Forests v. 12, n. 7, p. 958, 2021.

COSENZA, D. N.; SOARES, P.; GUERRA-HERNÁNDEZ, J.; PEREIRA, L.; GONZÁLEZ-FERREIRO, E.; CASTEDO-DORADO, F.; TOMÉ, M. Comparing Johnson's S_B and Weibull functions to model the diameter distribution of forest plantations through ALS data. Remote Sensing v. 11, n. 23, p. 2792, 2019.

DE LIMA, R. A. F.; BATISTA, J. L. F.; PRADO, P. I. Modeling tree diameter distributions in natural forests: an evaluation of 10 statistical models. Forest Science v. 61, n. 2, p. 320-327, 2015.

EZENWENYI, J. U.; OLADOYE, A. O.; CHUKWU, O.; BASIRU, A. O. Diameter distribution of *Nauclea diderrichii* (D Wild) Merr. plantations in a restricted tropical rainforest of Nigeria. Journal of Research in Forestry, Wildlife and Environment v. 10, n. 3, p. 25-32, 2018.

FONSECA, T. F. Modelação do crescimento, mortalidade e distribuição, do pinhal bravo no Vale do Tâmega. Ph.D. dissertation Univ. of Trás-os-Montes e Alto Douro, Vila Real, Portugal, 2004.

FONSECA, T. F.; MARQUES, C. P.; PARRESOL, B. R. Describing Maritime pine diameter distributions with Johnson's S_B distribution using a new all-parameter recovery approach. Forest Science v. 55, n. 4, p. 367-373, 2009.

FURTADO, A. X. Modelação da estrutura dinâmica de povoamentos de *Eucalyptus globulus* em primeira rotação. Tese de Doutoramento, Faculdade de Ciências e Tecnologia da Universidade Nova de Lisboa, 2006.

GENERAL DIRECTORATE OF FORESTRY. Available in: <https://www.ogm.gov.tr>, 2020.

GORGOSO-VARELA, J. J.; OGANA, F. N.; IGE, P. O. A comparison between derivative and numerical optimization methods used for diameter distribution estimation. Scandinavian Journal of Forest Research v. 35, n. 3-4, p. 156-164, 2020.

HAFLEY, W.; SCHREUDER, H. Statistical distributions for fitting diameter and height data in even-aged stands. Canadian Journal of Forest Research v. 7, n. 3, p. 481-487, 1977.

JOHNSON, N. L. Systems of frequency curves generated by methods of translation. Biometrika v. 36, n. 1-2, p. 149-176, 1949.

KAMZIAH, A. K. Development of diameter distribution yield prediction models for simulation of Acacia mangium plantations Doctoral dissertation, M. Sc. thesis, Univ. of Putra Malaysia, Malaysia, 1998.

KIVISTE, A.; NILSON, A.; HORDO, M.; MERENÄKK, M. Diameter distribution models and height-diameter equations for Estonian forests. Modelling Forest Systems, 2003, p. 169-179.

LEI, Y. Evaluation of three methods for estimating the Weibull distribution parameters of Chinese pine (*Pinus tabulaeformis*). Journal of Forest Science v. 54, n. 12, p. 566-571, 2008.

LIMA, R. B.; BUFALINO, L.; ALVES, F. T.; SILVA, J. A. D.; FERREIRA, R. L. Diameter distribution in a Brazilian tropical dry forest domain: Predictions for the stand and species. Anais da Academia Brasileira de Ciências v. 89, p. 1189-1203, 2017.

LIU, C.; BEAULIEU, J.; PREGENT, G.; ZHANG, S. Y. Applications and of six methods for predicting parameters of the Weibull function in unthinned *Picea glauca* plantations. Scandinavian Journal of Forest Research v. 24, n. 1, p. 67-75, 2009.

MALTAMO, M.; MEHTÄTALO, L.; VALBUENA, R.; VAUHKONEN, J.; PACKALEN, P. Airborne laser scanning for tree diameter distribution modelling: a comparison of different modelling alternatives in a tropical single-species plantation. Forestry: An International Journal of Forest Research v. 91, n. 1, p. 121-131, 2018.

MATEUS, A.; TOMÉ, M. Modelling the diameter distribution of eucalyptus plantations with Johnson's S_B probability density function: parameters recovery from a compatible system of equations to predict stand variables. Annals of Forest Science v. 68, n. 2, p. 325-335, 2011.

MAYRINCK, R. C.; FILHO, A. C. F.; RIBEIRO, A.; OLIVEIRA, X. M. D.; LIMA, R. R. D. A comparison of diameter distribution models for *Khaya ivorensis* A. Chev. plantations in Brazil. Southern Forests: A Journal of Forest Science v. 80, n. 4, p. 373-380, 2018.

MOWRER, H. T. ASPNORM: a normal diameter distribution growth and yield model for aspen in the central Rocky Mountains. USDA For Serv Res Pap RM US Rocky Mt for Range Exp Stn. Fort Collins, Colo.: The Station, (RM-IT-264), 1986.

NEWBERRY, J. D.; BURK, T. E. S_B distribution-based models for individual tree merchantable volume-total volume ratios. Forest Science v. 31, n. 2, p. 389-398, 1985.

NORD-LARSEN, T.; CAO, Q. V. A diameter distribution model for even-aged beech in Denmark. Forest Ecology and Management v. 231, p. 218-225, 2006.

OGANA, F. N.; ITAM, E. S.; OSHO, J. S. Modeling diameter distributions of *Gmelina arborea* plantation in Omo Forest Reserve, Nigeria with Johnson's S_B. Journal of Sustainable Forestry v. 36, n. 2, p. 121-133, 2017.

ÖZÇELIK, R.; CAO, Q. V.; KURNAZ, E.; KOPARAN, B. Modeling diameter distributions of mixed-oak stands in Northwestern Turkey. CERNE, v. 28, 2022.

ÖZÇELIK, R.; FIDALGO FONSECA, T. J.; PARRESOL, B. R.; ELER, Ü. Modeling the diameter distributions of Brutian pine stands using Johnson's S_B distribution. Forest Science v. 62, n. 6, p. 587-593, 2016.

PARRESOL, B. R. Recovering parameters of Johnson's S_B distribution. US Forest Service Research Paper 2003 SRS-31, 2003, p. 9.

PARRESOL, B. R.; FONSECA, T. F.; MARQUES, C. P. Numerical details and SAS programs for parameter recovery of the S_B distribution. US Forest Service General Technical Report SRS-122. USDA, USA, 2010, p. 27.

POGODA, P.; OCHAŁ, W.; ORZEŁ, S. Modeling diameter distribution of black alder (*Alnus glutinosa* (L.) Gaertn.) stands in Poland. Forests, v. 10, n. 5, p. 412, 2019.

POGODA, P.; OCHAŁ, W.; ORZEŁ, S. Performance of Kernel estimator and Johnson S_B function for modeling diameter distribution of black alder (*Alnus glutinosa* (L.) Gaertn.) stands. Forests v. 11, n. 6, p. 634, 2020.

REYNOLDS, M. R. J. R.; BURK, T. E.; HUANG, W. C. Goodness-of-fit tests and model selection procedures for diameter distribution models. Forest Science v. 34, n. 2, p. 373-399, 1988.

SAKICI, O. E. A Comparison of Diameter Distribution Models for Uneven-aged Kazdağı Fir Stands in Kastamonu Region of Turkey. Global Conference on Engineering Research, Türkiye, (02-05 June 2021), 2021.

SAKICI, O. E.; DAL, E. Modelling diameter distributions and determination of their relationships with some stand characteristics for Scots pine stands in Kastamonu region. Journal of Bartin Faculty of Forestry v. 23, n. 3, p. 1026-1041, 2021.

SAS INSTITUTE. SAS/OR(R) 9.2 User's Guide: Mathematical Programming. 2010. Available in: <https://support.sas.com/documentation/cdl/en/ormpug/59679/HTML/default/viewer.htm#optmodel.htm>, Access in August 2023.

SCOLFORO, J. R. S.; TABAI, F. C. V.; DE MACEDO, R. L. S. G.; ACERBI, F. W.; DE ASSIS, A. L. S_B distribution's accuracy to represent the diameter distribution of *Pinus taeda*, through five fitting methods. Forest Ecology and Management v. 175, n. 1, p. 489-496, 2003.

SCOLFORO, J. R. S.; THIERSCHI, A. Estimativas e testes da distibuiçao de frequencia diametrica para *Eucalytus camaldulensis*, através da distribuição S_B de Johnson, por diferentes métodos de ajuste. Forest Science v. 54, n. 1, p. 93-106, 1998.

SIIPILEHTO, J.; SIITONEN, J. Degree of previous cutting in explaining the differences in diameter distributions between mature managed and natural Norway spruce forests. Finnish Society of Forest Science Finnish Forest Research Institute. 2004.

SUN, S.; CAO, Q. V.; CAO, T. Characterizing diameter distributions for uneven-aged pine-oak mixed forests in the Qinling Mountains of China. Forests v. 10, p. 596, 2019.

VEGA, A. A.; CORRAL RIVAS, S.; CORRAL RIVAS, J. J.; DIÉGUEZ ARANDA, U. Modelling diameter distribution of natural forests in Pueblo Nuevo, Durango State. Revista Mexicana de Ciencias Revista Mexicana de Ciencias Forestales, v. 13, n. 73, p. 75-101, 2022.

ZHANG, L.; PACKARD, K. C.; LIU, C. A comparison of estimation methods for fitting Weibull and Johnson's S_B distributions to mixed spruce fir stands in northeastern North America. Canadian Journal of Forest Research v. 33, n. 7, p. 1340-1347, 2003.